

## Measurement of Fission Cross Section and Angular Distributions of Fission Fragments from Neutron-Induced Fission of $^{243}\text{Am}$ in the Energy Range 1 – 500 MeV

A.M. Gagarski<sup>1</sup>, A.S. Vorobyev<sup>1</sup>, O.A. Shcherbakov<sup>1</sup>, L.A. Vaishnena<sup>1</sup>,  
A.L. Barabanov<sup>2,3</sup>, T.E. Kuz'mina<sup>4</sup>

<sup>1</sup>NRC “Kurchatov Institute”, B.P. Konstantinov Petersburg Nuclear Physics Institute,  
188300, Gatchina, Leningrad district, Russia

<sup>2</sup>NRC “Kurchatov Institute”, 123182, Moscow, Russia

<sup>3</sup>National Research Nuclear University “MEPhI”, 115409, Moscow, Russia

<sup>4</sup>V.G. Khlopin Radium Institute, 194021, St.-Petersburg, Russia

Fission cross sections and angular distributions of fission fragments from the neutron-induced fission of  $^{243}\text{Am}$  have been measured in the energy range 1–500 MeV at the neutron time-of-flight spectrometer based on the neutron complex GNEIS at the 1GeV proton synchrocyclotron of the NRC “Kurchatov Institute” - PNPI (Gatchina). The description of the experimental set-up consisted of two MWPC counters with targets of  $^{243}\text{Am}$  and  $^{235}\text{U}$  is given, as well as the some principal details of experimental data processing.

The fission cross section of  $^{243}\text{Am}$  was obtained by ratio method using  $^{235}\text{U}$  as a standard. The anisotropy of fission fragments  $W(0^\circ)/W(90^\circ)$  was deduced from the experimental data on angular distributions of  $^{243}\text{Am}$ . The anisotropy data are of particular interest because in the investigated energy range 1–500 MeV other experimental data are practically absent, despite the ever-growing interest in this field, stimulated by the creation of new nuclear technologies. This work is a part of the program dedicated to investigations of neutron-induced fission at intermediate energies.

### Introduction

The data on nuclear fission in intermediate energy range 1–200 MeV are of prime importance for the advanced nuclear technologies such as Accelerator-Driven Systems (for nuclear power generation and nuclear transmutation). The information about angular distribution of fission fragment is also very important to verify parameters of theoretical models used for adequate fission process description in neutron energy range above 20 MeV. The systematic study of angular distributions of fission fragments is limited to that these experimental data are very scarce in neutron energy range above 20 MeV and are practically absent for neutron energy range above 100 MeV. Data on the angular distributions of fission fragments are important for accurate measurements of fission cross-sections, since they should be taken into account as an efficiency correction for detectors other than  $4\pi$ . There is no such data for  $^{243}\text{Am}$ , unless two data points of Fursov et al. [1] at the energy 2.5 MeV.

One of the main problems in the reprocessing of spent nuclear fuel produced in modern nuclear reactors are Am and Cm isotopes due to their high activity and long half-life. Am is the most dangerous due to its high yield and high activity.  $^{243}\text{Am}$  contributes also to the formation of  $^{239}\text{Pu}$ . The share of  $^{243}\text{Am}$  among other minor Am actinides is ~15% in spent fuel

from thermal reactors. Today, the transmutation of nuclear waste in fast neutron reactors seems to be one of the promising ways to reduce the radiotoxicity of spent nuclear fuel.

The practical implementation of plans for both the creation of a closed fuel cycle based on fast nuclear reactors and the disposal of radioactive waste is impossible without reliable and accurate nuclear data. For example, the required accuracy of the fission cross section of  $^{243}\text{Am}(n,f)$  is 7% when designing the sodium-cooled fast reactor (SFR) and 2% for designing the accelerator-driven minor actinide burner reactor (ADMAB) [2]

The data available on the fission cross section of  $^{243}\text{Am}$  are mainly limited to the neutron energies below 20 MeV [1, 3–11]. These data were obtained using both monoenergetic neutron beams and time-of-flight technique with “white” neutron spectrum at the pulsed accelerators (neutron sources) including nuclear explosion. The available experimental data reveals a significant scatter, which reaches 30% in the neutron energy range of 2–10 MeV (Fig.1).

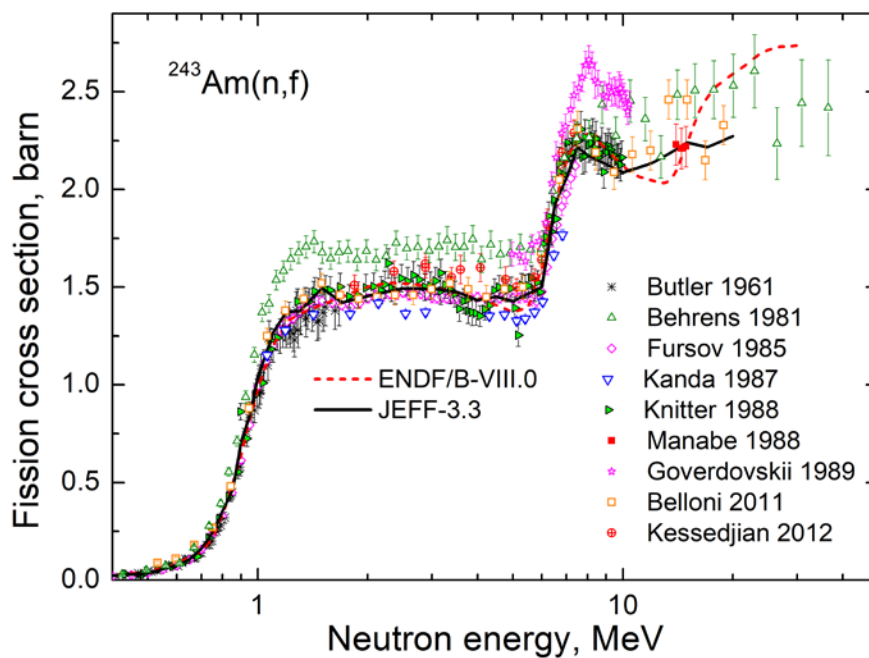


Fig. 1. The fission cross sections of  $^{243}\text{Am}$ .

The maximum deviation from the array of experimental data and estimated data from the ENDF/B-VIII.0 and JEFF-3.3 libraries are the experimental data of Behrens et al. [5] and Goverdovskii et al. [9]. These data on the  $^{243}\text{Am}$  fission cross sections were measured by the standard method relative to the  $^{235}\text{U}$  fission cross section, but absolute normalization was carried out using the threshold cross section method (Behrens et al.) and similar method of elemental impurities (Goverdovskii et al.) instead of accurately measuring the number of target nuclei  $^{243}\text{Am}$  and  $^{235}\text{U}$ . This circumstance, apparently, was the reason for the significant deviation of the data (Behrens et al. and Goverdovskii et al.) in absolute magnitude, while maintaining the shape of the cross-section curve in the above-threshold region of neutron energies. There are practically no experimental data for neutron energies above 20 MeV. Therefore, new measurements with absolute normalization of the fission cross section of  $^{243}\text{Am}$  should be made in a wide neutron energy range on neutron beams with a continuous spectrum using the time-of-flight method.

### General description of the experiment

The measurements were carried out at the 36 m flight path of the neutron TOF-spectrometer GNEIS based on the spallation neutron source at 1 GeV proton synchrotron SC-1000 of the NRC KI – PNPI (Gatchina, Russia) [12, 13]. The short pulse width 10 ns of the neutron source enables to carry out TOF-measurements with the energy resolution from 0.8% (at 1 MeV) to 13% (at 200 MeV). A detailed description of the set-up can be found in our previous publications [14–22]. The main features of the present measurements are described below.

The fission cross section of the nucleus under study was measured relative to the cross section of a reaction that is known with high accuracy (standard cross section), in present measurements, that is the neutron induced fission of  $^{235}\text{U}$ . To do this, it was necessary to prepare the target of  $^{243}\text{Am}$  and reference target of  $^{235}\text{U}$  with exactly known ratio of number of nuclei ( $N_{\text{Am3}}/N_{\text{U5}}$ ), to place these targets in the same neutron flux and to register fission fragments with detectors having the same (or well known) efficiencies.

The highly enriched targets of  $^{243}\text{Am}$  and  $^{235}\text{U}$  were manufactured at the JSC “V.G. Khlopin Radium Institute” (St. Petersburg, Russia). The isotopic compositions of the target materials are given in Table 1. The 0.1 mm thick aluminum foil was used as a substrate for

Table 1. Isotopic compositions of the targets

	$^{235}\text{U}$	$^{243}\text{Am}$
Isotope	Mass percentage (%)	
$^{235}\text{U}$	99.9920±0.0010	
$^{234}\text{U}$	0.0020±0.0005	
$^{236}\text{U}$	0.0040±0.0005	
$^{238}\text{U}$	0.0020±0.0005	
$^{243}\text{Am}$		99.13±0.10
$^{241}\text{Am}$		0.75±0.01
$^{244}\text{Cm}$		0.11±0.01

targets prepared by the “painting” technique. Table 2 provides information on geometry sizes of the targets, their total masses, areal densities and homogeneity, as well as target masses and activities. To ensure identical measurement conditions, circular areas of the same size were selected on the  $^{243}\text{Am}$  and  $^{235}\text{U}$  targets. To do this, identical 0.1 mm thick aluminum foil “masks” with a circle hole with a diameter of

48.0 mm were used, which were placed on the targets on the side of the active layer. To determine the masses of the substance in selected areas, the  $\alpha$ -activities measurements of the masked targets were carried out using semiconductor detector. The measured ratio of number of nuclei ( $N_{\text{Am3}}/N_{\text{U5}}$ ) was found with relative statistical uncertainty 1.7 %.

Table 2. Parameters of the targets

Main isotope	$^{235}\text{U}$	$^{243}\text{Am}$
Thickness of active layer ( $\mu\text{g}/\text{cm}^2$ )	203(11)	142(7)
Homogeneity of active layer	10%	10%
Sizes of active layer (mm)	50×100	Ø 82
Total target mass (mg)	10.15(51)	7.5(4)
Main isotope mass inside mask Ø48 mm (mg)	3.480(48)	2.484(25)
Target activity inside the mask Ø48 mm (Bq)	295	$2.92 \times 10^7$
Scaling factor ( $N_{\text{Am3}}/N_{\text{U5}}$ )	0.690(12)	

A general view of the experimental setup and data acquisition system is shown in Fig. 2. The setup for measuring fission cross sections and angular distributions of fission fragments (FF) consists of two low pressure gaseous coordinate-sensitive multiwire proportional counters (MWPC) D1 and D2. The counters D1 and D2 were placed close to the target in the beam, one after the other. The neutron beam axis came through the geometrical centers of the target and the MWPC's electrodes being perpendicular to them. Data acquisition system was based on two waveform digitizers Acqiris DC-270 with sampling rate of 500 MSamples/s. This system as well as the methods of digital processing of signals from FF detector used enabled to perform measurements in a wide interval of neutron energy with a zero dead time. Herewith, almost perfect separation between fission events and products of other reactions was achieved at a practically zero FF registration threshold. To demonstrate the quality of this separation, for nuclei under study the amplitude spectra of fission fragments are shown in Fig. 3 for all events and for “useful” fission events selected by means of the procedure described in [15].

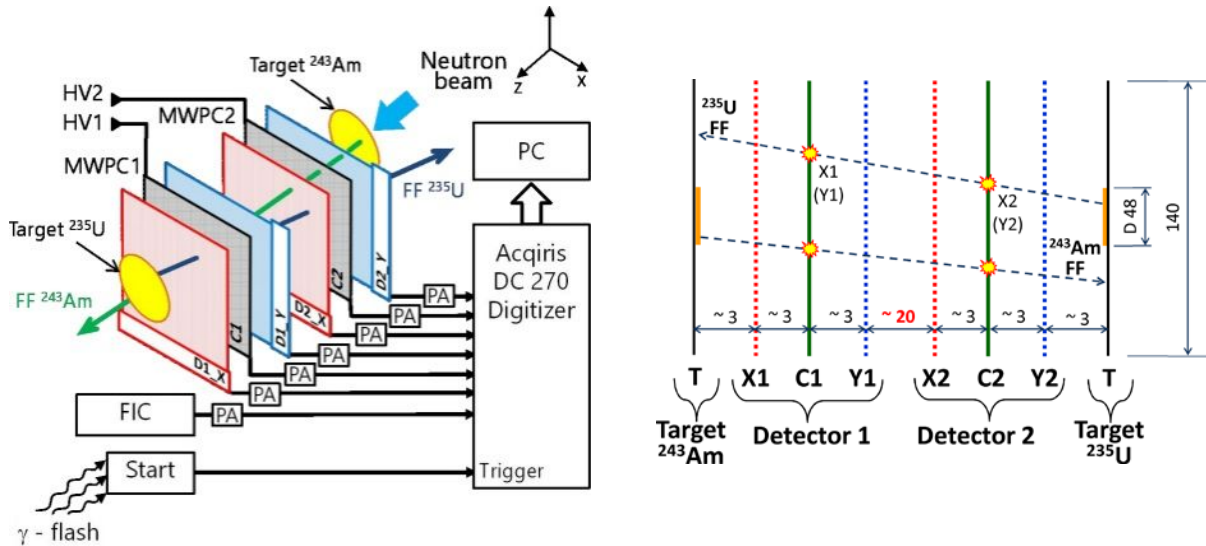


Fig. 2. Schematic view of the experimental setup and data acquisition system: left -Start - start detector; FIC - the fission ionization chamber with  $^{238}\text{U}$  targets (neutron flux monitor); PA – preamplifier; HV1, HV2 – high-voltage power sources; C1, C2 are the cathodes of MWPC1 and MWPC2, respectively; D1\_X, D2\_X – detectors 1,2 (X axis); anodes D1\_Y, D2\_Y – detectors 1,2 (Y axis); right – the internal structure of the MWPCs, the distances between electrodes and diameters are given in mm.

A small admixture of  $^{244}\text{Cm}$  in the  $^{243}\text{Am}$  target (0.11%) creates a background of spontaneous fission fragments. The background induced by spontaneous fissions of  $^{244}\text{Cm}$  was evaluated as  $305 \pm 9 \text{ min}^{-1}$ . It was calculated based on the efficiency of detection of fission fragments, the spontaneous fission half-life for  $^{244}\text{Cm}$ , and the mass of  $^{244}\text{Cm}$  in the “masked” target part, which was precisely determined in this work. Thus, at neutron energies about 200 keV the share of spontaneous fission in the total fission fragment counts rate was about 70%, and at energies above 1 MeV it does not exceed 0.2%. The spontaneous fission background was subtracted from the time-of-flight spectra and from the measured angular distributions of fission fragments.

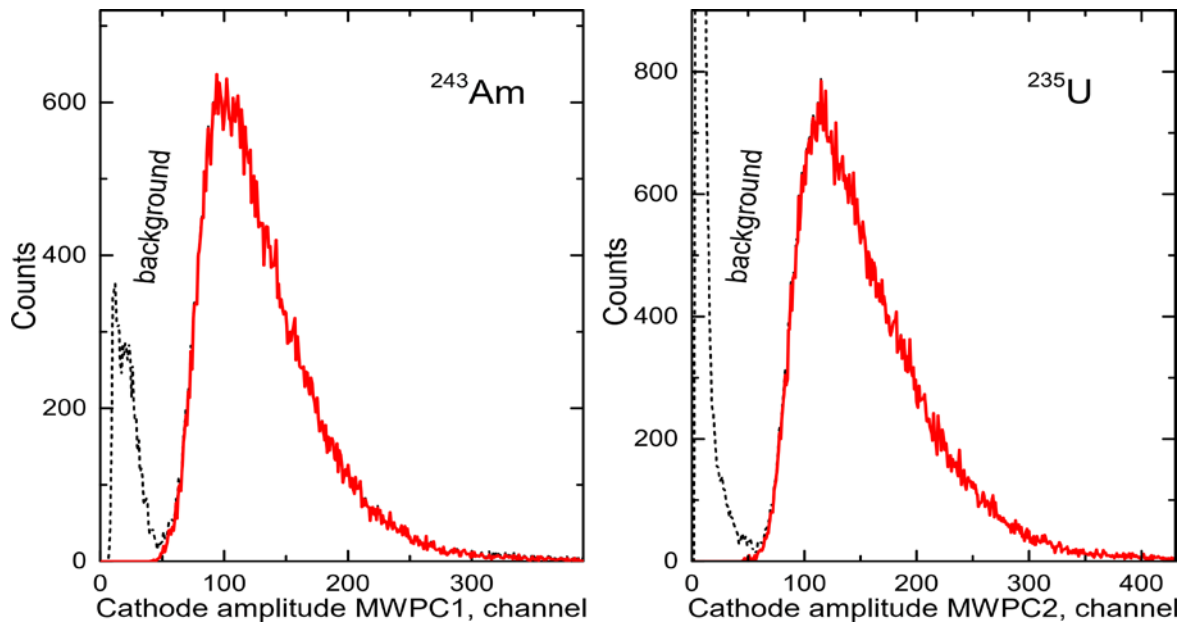


Fig. 3. The amplitude spectra of the signals from the MWPC cathode closest to the target of  $^{243}\text{Am}$  (left) and  $^{235}\text{U}$  (right), respectively. A continuous line indicates the spectrum obtained after the selection of “true” events, and a dashed line – before the selection.

The measured angular distributions for selected fission fragment events were corrected for the efficiency of fission fragment registration. This efficiency was calculated by means of the Monte-Carlo method taking into account the real geometry, design and features of the fission fragment detector the size of the active spot on the target separated by the “mask” and the spatial resolution of the MWPCs. The fission fragment detection geometrical efficiency was about 43%. The maximum fragment detection angle relative to the normal to the MWPC electrode plane was  $72^\circ$ . The obtained result is shown in Fig. 4.

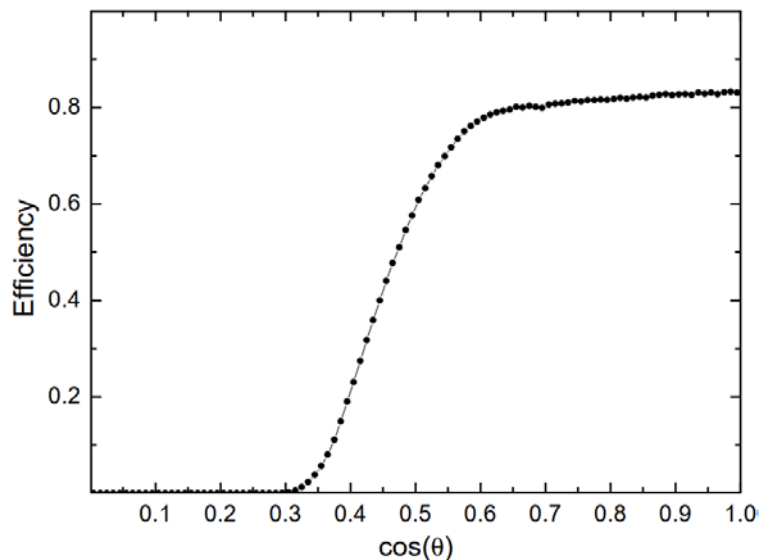


Fig. 4. The dependence of the efficiency of registration of fission fragments,  $\varepsilon$ , on the cosine of departure angle  $\theta$  relative to the normal to the target plane.

Note that the effect of momentum transfer from the incident neutron to the fissioning system on the angular distributions in the laboratory system should be taken into account. To determine this effect, angular distributions of fission fragments in the laboratory system were measured for two setup orientations relative to the beam direction (downstream and upstream). In the first, downstream, position, the beam direction coincides with the longitudinal momentum component of the detected fission fragment. In the second, upstream, position, the beam direction is opposite to the longitudinal momentum component of the detected fission fragment.

The angular distributions of fission fragments in the center-of-mass system were deduced from the corrected  $\cos(\theta)$  angular distributions in the laboratory system for two set-up orientations relative to the neutron beam direction ( $\cos(\theta)$  bins were equal to 0.01). Then, these distributions were fitted in the range  $0.35 < \cos(\theta) < 1.0$  by the sum of even Legendre polynomials up to the 4-th order and their anisotropy  $W(0^\circ)/W(90^\circ)$  was calculated using the coefficients  $A_2$  and  $A_4$  ( $A_0=1$ ) for the corresponding Legendre polynomials:

$$W(0^\circ) = A_0 \left[ 1 + \sum_{n=1}^2 A_{2n} P_{2n}[\cos(\theta)] \right]. \quad (1)$$

$$\frac{W(0^\circ)}{W(90^\circ)} = \frac{1 + A_2 + A_4}{1 - A_2/2 + 3A_4/8}. \quad (2)$$

### Results and discussion

The angular distributions of fission fragments for  $^{243}\text{Am}$  in the center of mass system for neutron energies 2.496 MeV and 14.95 MeV are shown in Fig. 5 together with the results of their fit. Fig. 6 displays the first experimental data on anisotropy of fission fragments for  $^{243}\text{Am}$  obtained in a wide neutron energy range for the first time. The systematic error in determining anisotropy in this experiment, which is related to the finite angular resolution of the arrays with MWPC and the uncertainty in the geometry of the experiment, is about 0.5%. The systematic error associated with the approximation used for fitting is 1–1.5%.

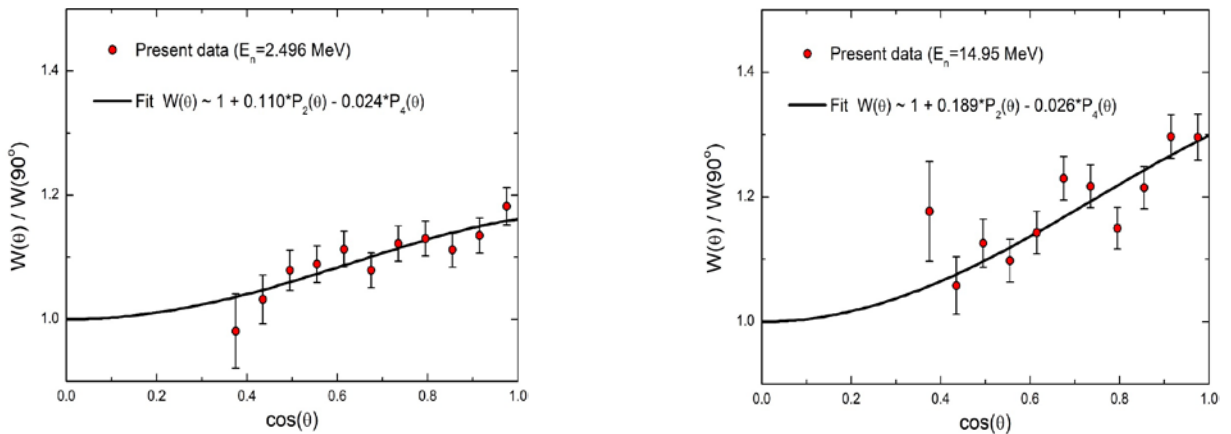


Fig. 5. Angular distributions of fission fragments for  $^{243}\text{Am}$ .

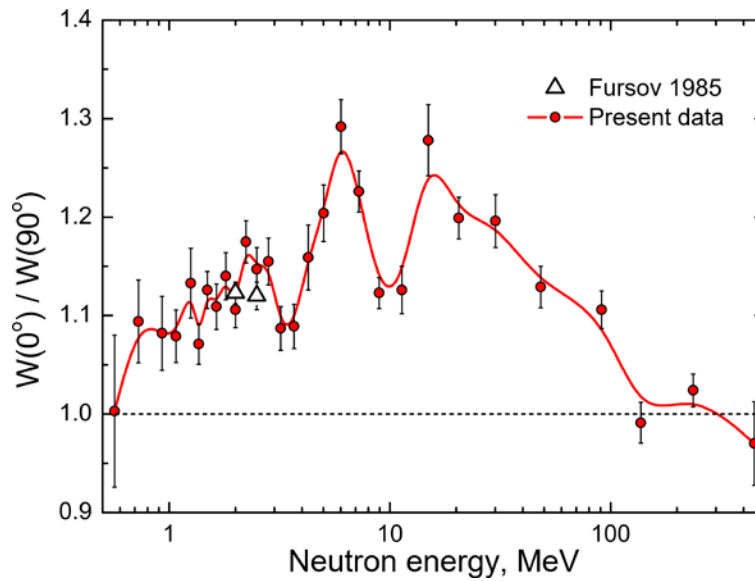


Fig. 6. Anisotropy of  $^{243}\text{Am}$  fission fragments in comparison with the data of Fursov et al. [1]. The error bars of present data represent total uncertainties. The solid curve is shown only for visualization of experimental data.

A new stage in experimental studies of the angular distribution of fission fragments began when the GNEIS team at NRC KI - PNPI, the n\_TOF collaboration at CERN and the NIFFTE collaboration at Los Alamos launched new experiments devoted to this problem almost simultaneously. The pulsed high-intensity sources of “spallation” neutrons of these facilities allow TOF-measurements of neutron-induced fission cross sections and angular distributions of fission fragments in the intermediate neutron energy range of 1–500 MeV. Two other important features of the experimental methods used by these research groups are the use of multichannel position-sensitive fission fragment detectors of varying degrees of complexity (MWPCs, PPACs, TPC) and the use of waveform digitizers for processing detector pulses. The results of these studies are presented in Table 3. Unfortunately, the results of measurements of the anisotropy of the  $^{235}\text{U}$  and  $^{238}\text{U}$  fission fragments obtained by the n\_TOF collaboration and published in the materials of the ND-2016 conference have not yet been presented in the EXFOR database.

The measured ratio of the neutron-induced fission cross sections of  $^{243}\text{Am}$  and  $^{235}\text{U}$  is shown in Fig. 7 together with the results of measurements performed by other authors [5–10, 23]. Digital data were taken from the EXFOR database. The experimental uncertainties of our ratio data are listed in Table 4. The statistical accuracy achieved in this work in the energy range above 1 MeV is 2–3% for a given energy bin. The total average systematic error is about 2% and is determined by the uncertainty in the thickness of the targets used (1.7%) and the anisotropy correction (1.0%).

Table 3. Status of experiments on angular distributions of fission fragment study

Nucleus	GNEIS, KI-PNPI	n-TOF, CERN	NIFFTE, WNR, LANL
<sup>232</sup> Th	JETP Lett.,102, 203(2015) EXFOR #41608002	Nucl. Data Sheets,119, 35 (2014) EXFOR #23209006	
<sup>233</sup> U	JETP Lett.,104, 365(2016) EXFOR #41616006		
<sup>235</sup> U	JETP Lett.,102, 203(2015) EXFOR #41608003 Phys. Rev. C 108, (2023) 014621, EXFOR #41757004	EPJ Web of Conf., 111 10002 (2016)	Phys. Rev. C 102, (2020) 014605, EXFOR #14660002 Phys. Rev. C 99, (2019) 064619, EXFOR #14606002
<sup>236</sup> U	Phys. Rev. C 108, (2023) 014621, EXFOR #41757001		
<sup>238</sup> U	JETP Lett.,102, 203(2015) EXFOR #41608004 JETP Lett.,117, 557(2023) EXFOR #41756002	EPJ Web of Conf., 111 10002 (2016)	Phys. Rev. C 102, (2020) 014605, EXFOR#14660003
<sup>237</sup> Np	JETP Lett.,110, 242(2019) EXFOR #416886002		
<sup>239</sup> Pu	JETP Lett.,107, 521(2018) EXFOR #41658003		
<sup>240</sup> Pu	JETP Lett.,112, 323(2020) EXFOR #41737002		
<sup>242</sup> Pu	Measurements completed		
<sup>243</sup> Am	Measurements completed		
<sup>nat</sup> Pb	JETP Lett.,107, 521(2018) EXFOR #41658004		
<sup>209</sup> Bi	JETP Lett.,104, 365(2016) EXFOR #41616007		

Table 4. Relative uncertainties for fission cross section ratio

Statistical uncertainties	
Counting statistic	60–3 % (0.2–1.0 MeV) 2–3 % (above 1.0 MeV)
Attenuation of the neutron flux	< 0.3 %
Anisotropy of fission fragments	1 %
Purity of targets (isotope composition)	1 % (below 0.8 MeV) 0.4 % (0.8–1.5 MeV) 0.1 % (above 1.5 MeV)
Efficiency of MWPC (geometrical uncertainty)	0.3 %
Scaling factor ( $N_{Am243}/N_{U235}$ )	1.7 %
Total error	3.2 %
Uncertainty of thr <sup>235</sup> U “standard” fission cross section	
$\sigma_f(^{235}\text{U})$	1.3–1.5 % (below 20 MeV) 1.5–4.8 % (2–200 MeV) 5–7 % (above 200 MeV)



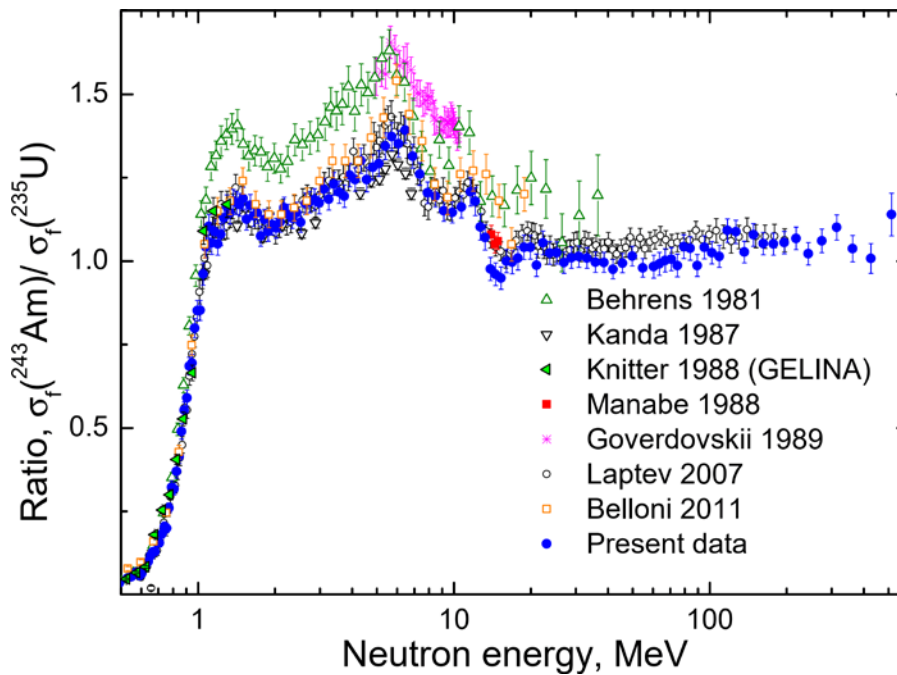


Fig. 7. Ratio of the fission cross sections of  $^{243}\text{Am}$  and  $^{235}\text{U}$ .

For neutron energies above 30 MeV, the ratio data obtained in this work can be compared only with the results of Laptev et al. [23]. It should be noted that the work of Laptev et al. was also performed at the GNEIS TOF-spectrometer using a multi-plate fission ionization chamber as a fission fragment detector. Unfortunately, in this work the measured ratio was not normalized to the number of nuclei in the targets. Instead, the authors normalized the ratio they obtained to the ratio of fission cross sections of  $^{243}\text{Am}$  and  $^{235}\text{U}$  taken from the ENDF/B-VII library for some neutron energy ranges. Nevertheless, it can be seen that, in general, there is good agreement between these and our present data over the entire neutron energy range studied.

It can be seen also that the  $^{243}\text{Am}$  fission cross section obtained in this work mostly agrees with the results of Kanda et al. [6], Manabe et al. [8], Belloni et al. [10] and Knitter et al. [7], obtained at the GELINA Linac using the TOF-method, while the data of Behrens et al. [5] and Goverdovskii et al. [9] are more than 15 % higher. Taking into account that the uncertainty of the scaling of the ratio stated in these works is only 2–3 %, one can talk about the presence of unknown systematic errors.

### Conclusion

In this work, new measurements of fission cross section and angular distributions of fission fragments for  $^{243}\text{Am}$  were carried out on the neutron TOF-spectrometer GNEIS at Petersburg Nuclear Physics Institute of National Research Centre “Kurchatov Institute” in the neutron energy range 0.3–500 MeV. The neutron induced fission cross section of  $^{243}\text{Am}$  was obtained in a wide energy range with the experimental uncertainty 3–4%. The data obtained on the fission cross section are mostly consistent with the results of earlier experimental works in the energy range up to 20 MeV, and above 20 MeV – the shape of the fission cross section agrees with the only existing old GNEIS data (Laptev et al. [23]). The differences between the existing experimental data seem to be mostly related to uncertainties in the detection efficiency of the fission fragment detectors used, the neutron flux and the target

masses (number of nuclei). The anisotropy of the angular distributions of  $^{243}\text{Am}$  fission fragments are measured in the energy range 0.7–400 MeV for the first time.

### Acknowledgments

The authors would like to thank the staff of the Accelerator Department of the NRC KI - PNPI for their permanent friendly assistance and smooth operation on the SC-1000 synchrocyclotron during the experiment, as well as L.S. Falev for help in creating the experimental setup.

### References

1. B.I. Fursov, E.Yu. Baranov, M.P. Klemyshev, B.F. Samylin, G.N. Smirenkin, Yu.M. Turchin, *Sov. At. En.* **59**, 899 (1985). EXFOR 40837003. EXFOR 40837006.
2. Nuclear Science/WPEC-26, Report NEA No. 6410, OECD-NEA, 2008.
3. D.K. Butler, R.K. Sjoblom, *Phys. Rev.* **124**, 1129 (1961). EXFOR 12543003.
4. P.A. Seeger, Los Alamos Sci. Lab. Rep. LA-4420, p.138 (1970). EXFOR 10063004.
5. J.W. Behrens, J.C. Browne, *Nucl. Sci. Eng.* **77**, 444 (1981). EXFOR 10652003.
6. K. Kanda, H. Imaruoka, H. Terayama, Y. Karino, N. Hirakawa, *Jour. of Nuclear Science and Technology* **24**, 423 (1987). EXFOR 22044002.
7. H. Knitter, C. Budtz-Jorgensen, *Nucl. Sci. Eng.* **99**, 1 (1988). EXFOR 22032002.
8. F. Manabe, K. Kanda, T. Iwasaki, H. Terayama, Y. Karino, M. Baba, N. Hirakawa, *Fac. of Engineering, Tohoku Univ. Tech. Report*, Vol. 52, Issue. 2, p. 97 (1988). EXFOR 22282009.
9. A.A. Goverdovskii, A.K. Gordyushin, B.D. Kuz'minov, V.F. Mitrofanov, A.I. Sergachev, S.M. Solov'ev, T.E. Kuz'mina, *Sov. At. En.* **67**, 524 (1989). EXFOR 41058002.
10. F. Belloni, M. Calviani, N. Colonna, P. Mastinu, P.M. Milazzo, U. Abbondanno, G. Aerts, H. Álvarez, F. Alvarez-Velarde, S. Andriamonje, *Eur. Phys. J. A* **47**, 160 (2011). EXFOR 23148002.
11. G. Kessedjian, G. Barreau, M. Aïche, B. Jurado, A. Bidaud, S. Czajkowski, D. Dassié, B. Haas, L. Mathieu, L. Tassan-Got, J.N. Wilson, F.-J. Hamsch, S. Oberstedt, I. AlMahamid, J. Floyd, W. Lukens, D. Shuh, *Phys. Rev. C* **85**, 044613 (2012). EXFOR 22993003, 22993004, 22993005.
12. N.K. Abrosimov, G.Z. Borukhovich, A.B. Laptev, V.V. Marchenkov, G.A. Petrov, O.A. Shcherbakov, Yu.V. Tuboltsev, V.I. Yurchenko. *Nucl. Instrum. Methods Phys. Res. A* **242**, 121 (1985).
13. O.A. Shcherbakov, A.S. Vorobyev, E.M. Ivanov. *Phys. Part. Nucl.* **49**, 81 (2018).
14. A.S. Vorobyev, A.M. Gagarski, O.A. Shcherbakov, L.A. Vaishnene, A.L. Barabanov. *JETP Letters* **102(4)**, 203 (2015).
15. A.S. Vorobyev, A.M. Gagarski, O.A. Shcherbakov, L.A. Vaishnene, A.L. Barabanov. *JETP Letters* **104(6)**, 365 (2016).
16. A.S. Vorobyev, A.M. Gagarski, O.A. Shcherbakov, L.A. Vaishnene, A.L. Barabanov. *JETP Letters* **107(9)**, 521 (2018).
17. A.M. Gagarski, A.S. Vorobyev, O.A. Shcherbakov, L.A. Vaishnene. In: “XXIII International Seminar on Interaction of Neutrons with Nuclei”, Dubna, May 25–29, 2015. JINR, E3-2016-12, 2016, p.73.

18. A.M. Gagarski, A.S. Vorobyev, O.A. Shcherbakov, L.A. Vaishnene. In: “XXIV International Seminar on Interaction of Neutrons with Nuclei”, Dubna, May 24–27, 2016. JINR, E3-2017-8, 2017, p.343.
19. A.S. Vorobyev, A.M. Gagarski, O.A. Shcherbakov, L.A. Vaishnene, A.L. Barabanov. In: “XXIV International Seminar on Interaction of Neutrons with Nuclei”, Dubna, May 24–27, 2016. JINR, E3-2017-8, 2017, p.413.
20. A.M. Gagarski, A.S. Vorobyev, O.A. Shcherbakov, L.A. Vaishnene, A.L. Barabanov. In: “XXV International Seminar on Interaction of Neutrons with Nuclei”, Dubna, May 22–26, 2017. JINR, E3-2018-12, 2018, p.342.
21. A.S. Vorobyev, A.M. Gagarski, O.A. Shcherbakov, L.A. Vaishnene, A.L. Barabanov. Proc. of the Int. Conf. “Nuclear data for Science and Technology ND-2016”, September 11–16, 2016, Bruges, Belgium. EPJ Web of Conferences **146**, 04011 (2017).
22. A.S. Vorobyev, A.M. Gagarski, O.A. Shcherbakov, L.A. Vaishnene, A.L. Barabanov. JETP Letters **110(4)**, 242 (2019).
23. A.B. Laptev, O.A. Shcherbakov, A.S. Vorobyev, R.C. Haight, A.D. Carlson, in Proceedings of the Conference on Fission and Properties of Neutron-Rich Nuclei, Sanibel Island (2007), edited by J.H. Hamilton, A.V. Ramayya, H.K. Carter (World Scientific, 2008) p. 462. EXFOR 41487015.